Lateral mobility of integral proteins in red blood cell tethers

David A. Berk and Robert M. Hochmuth

Department of Mechanical Engineering and Materials Science, Duke University, Durham, NC 27706

ABSTRACT   The red blood cell membrane is a complex material that exhibits both solid- and liquidlike behavior. It is distinguished from a simple lipid bilayer capsule by its mechanical properties, particularly its shear viscoelastic behavior and by the long-range mobility of integral proteins on the membrane surface. Subject to sufficiently large extension, the membrane loses its shear rigidity and flows as a two-dimensional fluid. These experiments examine the change in integral protein mobility that accompanies the mechanical phenomenon of extensional failure and liquidlike flow. A flow channel apparatus is used to create red cell tethers, hollow cylinders of greatly deformed membrane, up to 36-μm long. The diffusion of proteins within the surface of the membrane is measured by the technique of fluorescence redistribution after photobleaching (FRAP). Integral membrane proteins are labeled directly with a fluorescein dye (DTAF). Mobility in normal membrane is measured by photobleaching half of the cell and measuring the rate of fluorescence recovery. Protein mobility in tether membrane is calculated from the fluorescence recovery rate after the entire tether has been bleached. Fluorescence recovery rates for normal membrane indicate that more than half the labeled proteins are mobile with a diffusion coefficient of $\sim 4 \times 10^{-11}$ cm^2/s, in agreement with results from other studies. The diffusion coefficient for proteins in tether membrane is greater than 1.5×10^{-9} cm^2/s. This dramatic increase in diffusion coefficient indicates that extensional failure involves the uncoupling of the lipid bilayer from the membrane skeleton.

INTRODUCTION

The red blood cell membrane is a composite structure comprising a lipid bilayer with integral glycoproteins and an underlying cytoskeletal network of proteins including spectrin. Much progress has been made in recent years toward elucidating the biochemistry and microstructure of the cytoskeletal network (Bennett, 1985). This membrane skeleton endows the membrane with solidlike properties that are not characteristic of a simple lipid bilayer above the phase transition temperature. These solidlike properties are evident in mechanical studies of membrane deformation and in surface diffusion studies of integral membrane proteins.

Proteins inserted in the lipid bilayer of a biological membrane are subject to Brownian motion, and their rates of diffusion over macroscopic distances can be measured by the technique of fluorescence redistribution after photobleaching (FRAP). The mobility of these proteins in most membranes is limited not by the viscosity of the lipid bilayer, but by cytoskeletal constraints (Webb et al., 1981). It is clear that the measured rates of lateral diffusion are sensitive to the state of cytoskeletal structure. Sheetz et al. (1980) established that the diffusion coefficient of certain integral proteins in mouse erythrocytes is increased 50-fold in cells that are hereditarily deficient in the structural protein spectrin. Chemical factors that modify the cytoskeleton create measurable changes in the lateral mobility of glycoproteins in the red cell membrane (Golan and

Veatch, 1980; Schindler et al., 1980; Smith and Palek, 1982).

The mechanisms for this cytoskeletal control of lateral mobility are not yet fully understood. One theory holds that the spectrin matrix underlying the bilayer membrane presents transient barriers to the motion of integral proteins (Koppel et al., 1981). Long range protein motion would thus represent percolation through a dynamic network (Saxton, 1989).

Regardless of the mechanism, it is clear that the measurement of protein lateral mobility on the cell surface can be regarded as a probe of membrane structure. A rapid rate of protein diffusion, comparable to that of lipid molecules in the same membrane, can be interpreted as evidence of the destruction or uncoupling of the cytoskeleton from the lipid bilayer.

Just as the spectrin skeleton is the membrane component that constrains protein lateral mobility in the lipid bilayer, so is it the component that determines the mechanical shear deformation of the membrane. Shear deformation is equivalent to the elongation of an element of membrane with an attendant shortening in width so that the total surface area of the element is unchanged. For a lipid bilayer, deformation will continue indefinitely as long as the elongating force is applied. But for a red cell membrane complete with its superficial protein skeleton, the extent of elongation is limited and proportional to the magnitude of the elongat-

ing force. The constant of proportionality between force and deformation is the shear elastic modulus, a direct measure of membrane rigidity. Studies of spectrin-deficient erythrocytes indicate that the shear elastic modulus is proportional to the membrane's spectrin density (Waugh and Agre, 1988). The viscosity associated with shear deformation likewise reflects energy dissipation within the cytoskeletal mesh (Evans and Hochmuth, 1976a).

The erythrocyte membrane can undergo remarkable deformations while still maintaining its shear elastic nature, but when the local strain becomes sufficiently large the underlying membrane skeleton evidently loses its integrity and allows the membrane material to flow like a liquid. This liquidlike or inelastic behavior is observed in the formation of red cell "tethers": If a red cell becomes firmly attached at a point to a foreign surface and then experiences a sufficiently strong detachment force, the cell will move away from the surface still attached by a thin, cylindrically-shaped strand of membrane material called a tether. During this process membrane material flows from the cell body onto the growing tether.

The tether phenomenon presents an excellent opportunity to probe membrane structure and gain a better understanding of membrane failure. Evans and Hochmuth (1976b) analyzed this extensional failure and flow process by applying a theory for the viscoplastic flow of a two-dimensional Bingham material. An apparent plastic viscosity has been measured with flow channel experiments (Hochmuth et al., 1976; Waugh, 1982) and with a micropipet technique (Hochmuth and Evans, 1982; Hochmuth et al., 1982). The interpretation of these results has been hampered by a lack of a model to describe the structural changes that accompany membrane extensional failure.

During the event of tether formation, the membrane structural protein matrix must accommodate enormous extensions as membrane is stretched from its original geometry into a long, thin cylinder. Fig. 1 summarizes some possible means for this accommodation. During elastic deformation, the lipid bilayer and the cytoskeleton are securely coupled. The cytoskeleton may rearrange significantly so that the tether membrane maintains the normal structure as it flows (Fig. 1 a). This rearrangement might be similar to the structural changes that occur when a normally elastic deformation is imposed over a long period of time (Markle et al., 1983). Alternatively, the extensional flow process could involve the fragmentation of the cytoskeletal network with no subsequent rearrangement into a normal network (Fig. 1 b). A final possibility is that the lipid bilayer is completely separated from the protein network, creating
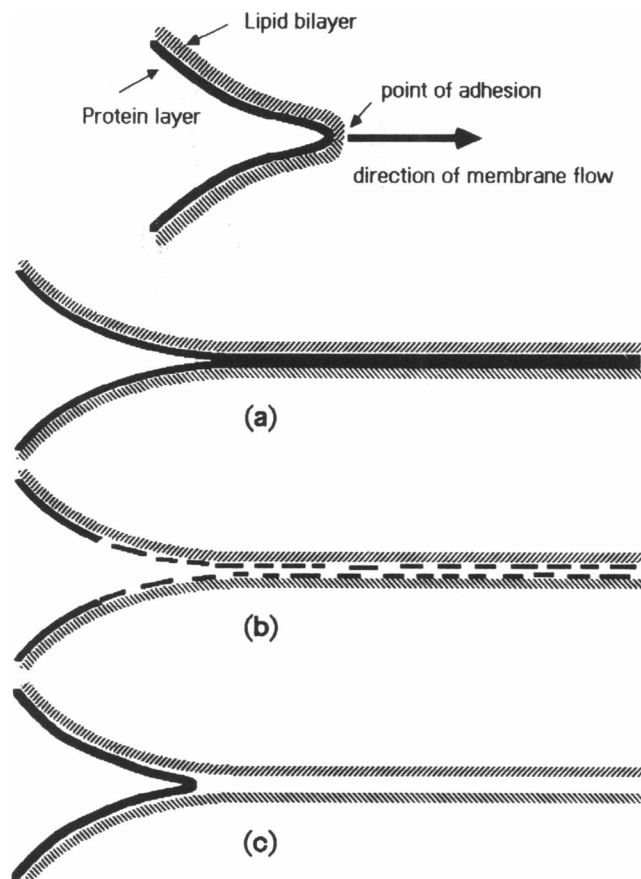

FIGURE 1 Formation of a membrane tether. The initial protrusion at the point of adhesion occurs elastically. When the extending force is great enough, membrane flows from the cell body onto the cylindrical tether. The solidlike protein network accommodates this flow by (a) extensively rearranging to form a new intact network, (b) fragmenting into an unorganized layer devoid of structural integrity, or (c) extending only slightly whereas the lipid bilayer separates and flows over the protein network.

a tether that consists solely of a lipid bilayer and integral membrane proteins, devoid of the superficial proteins.

The goal of these experiments has been to measure protein diffusion in the red cell tether and, in doing so, characterize the structure of extensionally failed membrane. Mechanical methods are not adequate to distinguish whether a tether membrane contains an elastic protein network or just a bilayer because even the liquidlike lipid bilayer has a curvature elasticity which causes it to exhibit elastic behavior when formed into a tether (Waugh and Hochmuth, 1987). Therefore, we have attempted to measure surface diffusivity to probe the structure of the tether membrane. Based on the previously mentioned studies of mobility in intact and cytoskeletally deficient membrane, the diffusion coeffi-

cient for integral proteins on the tether membrane is clearly an indicator of the membrane structure.

In our experiments, tethers are extracted from red cells whose integral proteins are fluorescently labeled with dichlorotriazinylaminofluorescein (DTAF). The entire tether surface is photobleached, and the fluorescence of the tether as a whole is monitored as new fluorescent particles diffuse from the cell body onto the tether. The FRAP technique used here is similar to the original experiments of Peters et al. (1974) in that instead of a laser a conventional mercury vapor arc lamp is used as the photobleaching and fluorescence excitation light source. To verify that the fluorescence recovery depends primarily on diffusion on the tether surface rather than on the cell body, we have developed a mathematical solution that describes diffusion from a spherical cell surface to a cylindrical projection or tether. The solution is presented in detail in a companion paper (Berk et al., 1992) and summarized below.

MATERIALS AND METHODS

Fluorescent labeling

A 0.5-ml sample of human blood is collected by finger prick and washed once in HEPES-buffered saline (132 mM NaCl, 4.7 mM KCl, 2.0 mM $CaCl_2$, 1.2 mM $MgSO_4$, 20 mM HEPES, adjusted to pH 7.4). The packed cells are then washed once in 145 mM NaCl − 10 mM $NaHCO_3$, pH 9.5, and resuspended in the same buffer with 1 mg/ml DTAF (obtained from Research Organics, Cleveland, Ohio). The cells are incubated on ice for 1 h, then washed twice in 50 mM glycine − 95 mM NaCl − 10 mM $NaHCO_3$, pH 9.5, to remove any dye that has not bound covalently to protein. Finally, the cells are washed twice and resuspended to ~2% hematocrit in HEPES-buffered saline with 1 mg/ml bovine serum albumin.

Tether formation

Membrane tethers are extracted from erythrocytes by the method of Hochmuth et al. (1973). A special flow chamber allows the application of fluid shear force to the cells while they are being viewed under a microscope. A channel is formed by a Parafilm (American Can Co., Neenah, WI) gasket sandwiched between a rectangular glass cover slip and a plastic slide with drilled entrance and exit holes. An infusion pump (model 906, Harvard Apparatus, South Natick, MA) injects saline solution through the channel at a controlled rate. The temperature of the infused solution is monitored and found to be at the ambient temperature of 27°C ± 1°C. After the red cell suspension is injected into the chamber, the cells are allowed to sediment. The infusion pump is then activated, and the cells that have not adhered to the coverslip are flushed away by the flow of saline solution. Red blood cells will adhere readily to naked glass, but due to the presence of albumin in the infusing solution the coverslip acquires a protective coating that prevents excessive sticking. Those cells that are attached to the glass surface elongate as the fluid shear force causes elastic deformation of the membrane. The flow rate is increased until a point-attached cell is observed to move several cell lengths downstream, an indication that a tether has formed between the cell and its point of attachment. The tether itself is only faintly visible because its

diameter is close to the wavelength of light. Once the tether has formed, the flow rate is reduced and adjusted so that the flow of membrane from cell body to tether ceases. The cell body maintains its new position and eventually adheres again to the glass surface. Fig. 2 shows a video image of elongated and tethered red blood cells.

Optics and electronics

Fig. 3 is a schematic of the optical and electronic system that performs the FRAP experiment. The flow chamber is mounted on the stage of a Leitz Diavert (Rockleigh, NJ) inverted microscope equipped for incident-light fluorescence microscopy. The dichroic mirror and excitation/emission filters are the standard combination for use with fluorescein dyes (Leitz designation I2), with excitation wavelength in the range 450–490 nm. The objective is an oil immersion type with 100× magnification and 1.25 numerical aperture. A 100 watt high pressure mercury arc lamp (Osram, Munich) with an appropriate power supply and housing (Oriel, Stamford, CT) serves as the fluorescence excitation source. A computer-controlled electronic shutter (Vincent Associates, Rochester, NY) limits the exposure duration and is synchronized with a photon-counting electronic system for measuring fluorescence intensity. The field diaphragm of the incident light illuminator is used to limit excitation to a circular area of diameter 20–40 μm.

The tether formation process is observed under transmitted light illumination (a separate light source, not shown in the figure) with a low-intensity monochromatic (577 nm) light to avoid premature photobleaching of the fluorescein dye. After a suitable tether has been identified, the microscope stage is adjusted to place the tether completely within the field of incident light illumination while the cell body remains outside this field. A narrow slit aperture is positioned
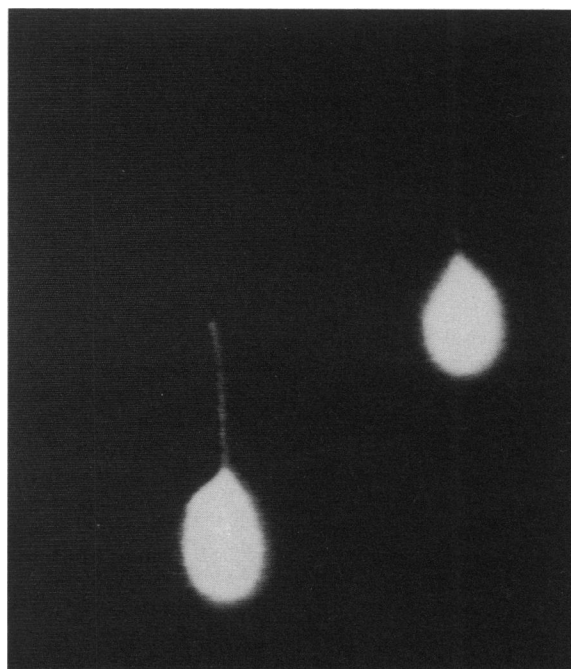

FIGURE 2 Video image of fluorescent cells in the flow channel. The flow is from top to bottom in this photograph. The bright fluorescence makes the tether appear thicker than its actual diameter. In transmitted light it is barely visible.
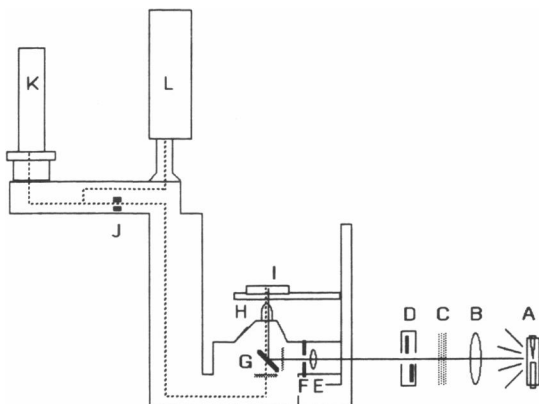
FIGURE 3 Optical system for fluorescence measurement and photo-bleaching. Light from a high pressure mercury arc lamp (*A*) passes through a collecting lens (*B*) neutral density filter (*C*) (typically 0.5 optical density), an electronic shutter (*D*), into the epi-illuminator of an inverted microscope, through a focusing lens (*E*), field diaphragm (*F*), and dichroic mirror/filter combination (*G*). The oil immersion objective (*H*) collects the excited fluorescence light from the sample (*I*), and the fluorescent image passes through a slit aperture (*J*) and is divided between a photomultiplier tube (*K*) and a low-light-level video camera (*L*). Photon counting electronics and video processing are discussed in the text.

within the image plane to block out stray light and isolate the tether for fluorescence measurement (Fig. 3 *J*). At this point, the transmitted light source is blocked, and the computer-controlled fluorescence measurement and photobleaching routine is activated.

At regular intervals, an output pulse from the microcomputer (PC model, IBM, Boca Raton, FL, equipped with a data acquisition board from Tecmar, Cleveland, Ohio) causes the shutter to open for a typical duration of 20 ms. Light from the brief fluorescent image is split with a series of prisms so that half the light is directed to a low-light-level SIT video camera (Model 66-SIT, Dage-MTI, Michigan City, IN) and half to a photomultiplier tube (Model 8850, RCA, Harrison, NJ) enclosed in an ambient temperature housing (Model PR1400RF, Products for Research, Danvers, MA). During the time that the electronic shutter is open, a video image processor (Model 794, Hughes Aircraft, Carlsbad, CA) is triggered to acquire the fluorescent image, providing a video snapshot that can be monitored to ensure that the subject remains in focus and that no foreign object intrudes into the field of view. A videotape recording of the image can be analyzed later to measure the tether length. Distances on the video screen are measured with a video caliper and calibrated by comparison with the video image of a stage micrometer. Also during the time the shutter is open, the photomultiplier signal is processed with the photon-counting technique. An amplifier/discriminator (Model AD6, Pacific Instruments, Concord, CA) generates a digital logic pulse for each signal pulse above a given magnitude, and those digital pulses are counted on a 100-MHz gated counter (Model 770, EG&G Ortec, Oak Ridge, TN). The microcomputer controls the gating, resetting, and recording of the photon count.

A typical experiment consists of a number of preliminary fluorescence measurements made during brief (20 ms) pulses of excitation light, followed by an extended period of illumination (typically 30 s) during which the tether is bleached, followed by another series of brief exposures, every 15–30 s, until the tether fluorescence appears to have completed its recovery.

Data analysis

A large part of the recovery process obeys a single exponential equation:

$$\frac{F_\infty - F(t)}{F_\infty - F_0} = \exp(-t/T). \tag{1}$$

The data are *t*, the time after the end of the photobleaching exposure, and *F*(*t*), the fluorescence intensity. These are fit to Eq. 1 using a three parameter least-squares fit. F_0 and F_∞ are the best-fit values for the bleached and steady-state intensities, and *T* is the recovery time constant from which the tether surface diffusion coefficient must be calculated. From the prebleach intensity F_i, and from F_0 and F_∞, the extent of recovery can be calculated:

$$\%R = \frac{F_\infty - F_0}{F_i - F_0} \times 100\%. \tag{2}$$

Because of the small signal/noise ratio in the measurements of tether fluorescence intensity, the correlation coefficients for these least-squares curve-fits are relatively low, despite the fact that the curves are obviously of the exponential sort predicted. Correlation coefficients between 0.80 and 0.95 correspond to good curve fits. The use of a higher order model with two exponential time constants did not appreciably improve the correlation. The relatively large amount of noise in the measurements means that the use of a model more complex than Eq. 1 is not justified.

CALCULATION OF THE DIFFUSION COEFFICIENT

In general, the rate of diffusion of fluorescent particles from the cell body onto the tether surface depends on the dimensions and diffusivities of both surfaces. An analysis of surface diffusion from a spherical shell to a cylindrical process is given in a separate paper (Berk et al., 1992). A large portion of the fluorescence recovery curve is described by a single exponential time constant:

$$T = \frac{1}{\sigma^2} \frac{L^2}{D_T}, \tag{3}$$

where σ is the smallest root of

$$\sigma \tan \sigma = \beta, \tag{4}$$

and

$$\beta = \frac{D_C}{D_T} \frac{L}{R_T \ell n(2R_C/R_T)}. \tag{5}$$

L is the tether length, D_T and D_C are the tether and cell body diffusion coefficients respectively, and R_T and R_C are the tether and cell body radii. When β is small, the rate-limiting step for fluorescence recovery is diffusion on the cell body and *T* is independent of D_T. When β is of order unity, the tether membrane offers significant resistance to diffusion, and for large β ($\beta \geq 25$) the tether is effectively the sole source of resistance to fluorescence recovery. In the case of a large value for β, σ approaches a value of $\pi/2$ and the time constant is a function only of the tether length and the tether diffusion coefficient.

Given measured or nominal values for the cell diffusion coefficient, cell radius, tether length, and tether radius, the tether diffusion coefficient can be determined by the use of Eqs. 3–5. In light of the

uncertainties in the values of D_C and R_T, it desirable as well to calculate the lower limit for the tether diffusion coefficient. By ascribing the entire delay in fluorescence recovery to the tether surface (i.e., $\beta \rightarrow \infty$) the minimum possible diffusion coefficient can be calculated:

$$D_{T,min} = \frac{4}{\pi^2} \frac{L^2}{T}. \qquad (6)$$

For a particular tether fluorescence recovery experiment, the length and the recovery time constant are measured quantities. Cell body radius is not measured directly because in these experiments the cell body is somewhat flaccid and tear-drop shaped. Instead, R_C is assigned a value of 3.4 μm, the radius of a sphere with the same surface area as a typical red cell. Because R_C appears only in a logarithmic term (Eq. 5), the solution is insensitive to variations in this particular parameter. On the other hand, the value of R_T, the tether radius can be quite critical in calculating the diffusion coefficients from the time constant. The tether radius cannot be measured directly because it is below the limits of resolution of the light microscope. Hochmuth et al. (1982, 1983) used a sensitive mechanical technique to measure radii for tethers extracted from spherical red blood cells subjected to membrane isotropic tensions between 0.2 and 0.4 dyne/cm. Larger tether radius resulted from lower isotropic tension, and extrapolation of the data to zero isotropic tension indicates that the tethers extracted from flaccid cells as in the present work should have a radius of at least 25 nm. Electron micrographic studies of tethers extracted from flaccid cells in flow channels place the tether radius in the range 45 to 65 nm (B. Wattenberg, R. Hochmuth, and J. Williamson, Washington University, unpublished observations; R. Waugh, personal communication). A nominal value of R_T = 50 nm is assigned as the best estimate.

Theoretically, the diffusion coefficient for the cell body can be calculated from the recovery data, but given the uncertainty in the value of R_T, this has not proven practical. Instead, D_C is taken to be ~4 × 10⁻¹¹ cm²/s. This value is chosen on the basis of published measurements of protein diffusion on the red cell surface (Sheetz et al., 1980) and on the basis of our own measurements. We measured the diffusion coefficient on the cell body with a technique similar to that of Peters et al. (1974) in which half the cell body is bleached by the light of the arc lamp and the subsequent fluorescence redistribution is monitored. The time constant that describes most of the return of fluorescence to the bleached half is given by (Huang, 1973):

$$T = \frac{R_C^2}{2 D_C}. \qquad (7)$$

The procedure for measurement of diffusion on the cell body surface is almost identical to the procedure for measurement of tether diffusion. A tether is extracted from a cell by the flow channel method and the cell is allowed to adhere again to the glass substrate. Then the cell is positioned so that half the body lies within the illuminated portion of the stage. The photobleach and subsequent fluorescence recovery of that half of the body is then observed.

RESULTS

Compared to the laser spot-bleach FRAP techniques, the half cell bleach method for measuring the diffusion coefficient on the cell body is unwieldy and less reliable. Nevertheless the results are consistent with the various published results for spot bleach and cell fusion experiments (Sheetz et al., 1980; Golan and Veatch, 1980;

Fowler and Branton, 1977; Schindler et al., 1980). Many of the cell bodies experienced morphological changes during the course of the experiment, namely the formation of echinocytes and spherocytes. As discussed below, this is thought to be the result of mechanical or chemical damage to the membrane. These damaged cells appeared to have a very low mobile fraction, and fluorescence recovery was not detected. For eight morphologically normal cells investigated by half-cell photobleach and recovery, the average cell body diffusion coefficient is 4 × 10⁻¹¹ cm²/s with a standard deviation of 2 × 10⁻¹¹ cm²/s. The extent of recovery ranges from 20% to 55%, which implies a mobile fraction of 40% to 100% of the labeled proteins on the red cell surface.

The 26 tethers studied range in length from 2 to 36 μm. The time constant of fluorescence recovery is on the order of several hundred to 1,000 s. Data from the shorter tethers (L < 10 μm) is not used to calculate D_T, because those recoveries were judged to be affected or even dominated by diffusion on the cell body (based on Eq. 5). The fluorescence signal is proportional to the tether length and the extent of the recovery: short tethers and those that recover only a small fraction of initial fluorescence tend to have a very small signal/noise ratio which makes it difficult to reliably determine the recovery time constant.

A total of 18 tethers were longer than 10 μm. Of those, ten recoveries are judged particularly good fits of the regression line to the data (primarily because of a higher signal/noise ratio for this data). The fluorescence intensity data from one experiment is presented in Fig. 4. The 21 μm tether is bleached and recovers 100% of its initial intensity with a time constant of T = 1,200 s. After a second photobleaching, the recovery is limited to 40%. Fig. 5 summarizes the data from all tethers longer than 10 μm. On the basis of Eq. 3, recovery time constants are scaled by the square of tether length.

Whereas the scaled recovery times are fairly consistent, there is much variability in the extent of recovery. There is evidence to suggest that incomplete recovery of tether fluorescence may reflect a loss of protein mobility on the cell body surface, not on the tether surface. Cells with <50% tether fluorescence recovery are observed to have rigid, spherical cell bodies rather than the flaccid, teardrop-shaped bodies they possessed prior to the experiment. This is the case, for example, for the recovery results shown in Fig. 4. After the second, incomplete recovery, inspection in transmitted light of the cell body revealed an apparent loss of surface area, resulting in the formation of a small ($R_C \approx 2$ μm) spherical cell body with a mottled appearance. The reason for this transformation from a flaccid tear-drop shape to a small rigid sphere was not established, except to note that the number of cells with this appearance
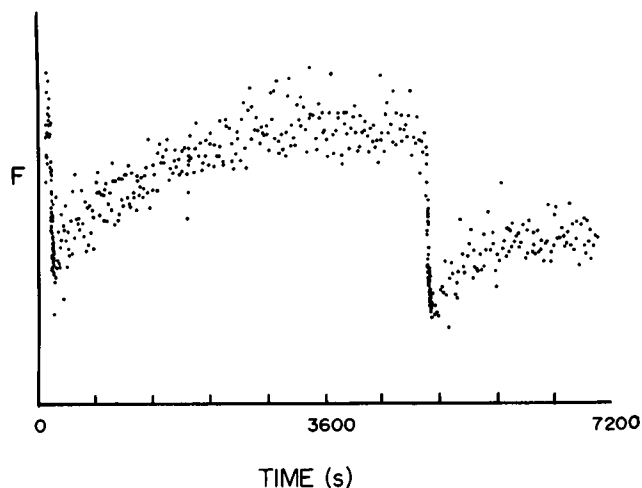
FIGURE 4 Photobleaching and fluorescence recovery for one 21-μm long tether. The tether recovers 100% of its initial intensity with a time constant of 1,200 s. After a second photobleaching, the tether recovers only 40% of initial intensity with a time constant of 500 s. Subsequent examination revealed a damaged cell body.

increases with time of exposure to fluid flow in the channel, even in the absence of the intense fluorescence excitation illumination. The phenomenon may be related to photodamage from the transmitted light illumination, to mechanical damage from the fluid shear stress, or to chemical effects of contact with the glass surface. Photobleaching experiments performed on the body of such a rigidified cell detect no mobility at all, but when half the cell's tether is bleached the tether regains a more uniform fluorescence. (Although the final fluorescence intensity profile of the tether appeared uniform to the eye, we lacked the facility for quantitating the spatial fluorescence distribution.)

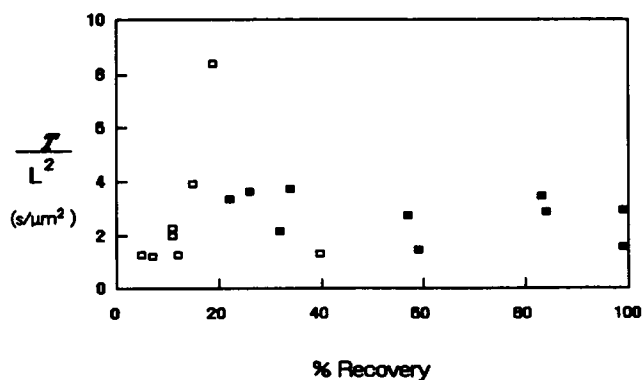The lower limit to the diffusion coefficient on tether

FIGURE 5 Summary of fluorescence recovery data for 18 tethers with lengths from 10 to 36 μm. Filled squares indicate the "good fit" recoveries with correlation coefficients higher than 0.80.

membrane, based on the ten good fit recoveries, is:

$$D_{\mathrm{T,min}} = 1.5 \times 10^{-9} \, \mathrm{cm}^2/\mathrm{s}.$$

The standard deviation is $0.6 \times 10^{-9} \, \mathrm{cm}^2/\mathrm{s}$.

When Eqs. 3–5 are used to obtain a better estimate of tether diffusivity, the calculation of D_{T} is sensitive to the values of R_{T} and D_{C}, tether radius and cell-body diffusion coefficient. If the cell body surface is assigned a diffusivity of $4 \times 10^{-11} \, \mathrm{cm}^2/\mathrm{s}$, then the average value for the tether surface is

$$D_{\mathrm{T}} = 4 \times 10^{-9} \, \mathrm{cm}^2/\mathrm{s},$$

and the standard deviation is 0.8×10^{-9}. The true tether radius may be closer to 50 nm, but in that case the recovery time constants shown in Fig. 5 are too fast to be compatible with $D_{\mathrm{C}} = 4 \times 10^{-11} \, \mathrm{cm}^2/\mathrm{s}$. If the cell body is assigned a diffusivity of $D_{\mathrm{C}} = 6 \times 10^{-11} \, \mathrm{cm}^2/\mathrm{s}$, then the average tether diffusion coefficient is.

$$D_{\mathrm{T}} = 6 \times 10^{-9} \, \mathrm{cm}^2/\mathrm{s},$$

with a standard deviation of 1×10^{-9}.

Fig. 6 illustrates the dependence of the calculated diffusion coefficient on the two parameters of tether radius and cell body diffusion coefficient. The average
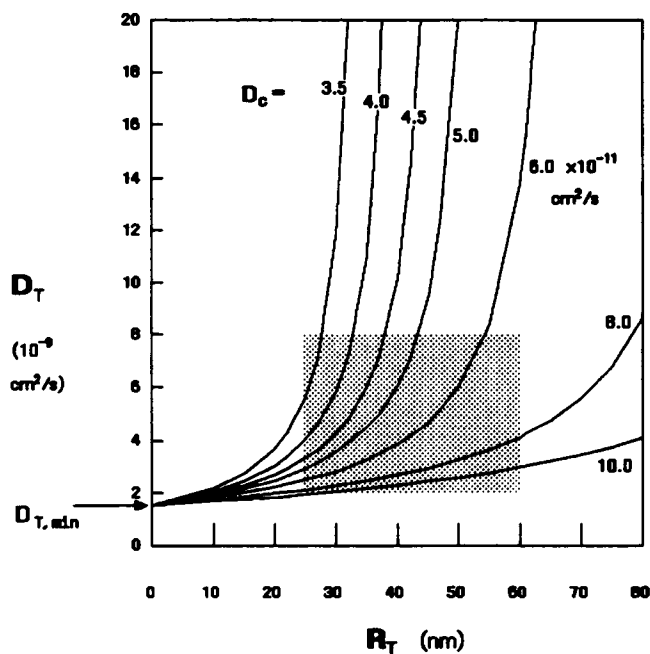

FIGURE 6 The calculated tether diffusion coefficient depends on the values of tether radius and cell-body diffusivity. For any combination of values for R_{T} and D_{C}, the average value for D_{T} is chosen to fit the 10 best sets of recovery data. The shaded region corresponds to the expected range of R_{T} and D_{T} ($> D_{\mathrm{T,min}}$ but less than the lipid diffusion coefficient).

tether diffusion coefficient calculated from ten fluorescence recovery experiments is plotted as a function of tether radius and for different values for cell-body diffusivity. For thin tethers and fast diffusion on the cell body, the calculated value of D_T is close to the lower limit given by Eq. 6, $D_{T,min} = 1.5 \times 10^{-9}$ cm^2/s. For increasing values of R_T and decreasing values of D_C, the calculated average tether diffusivity becomes very sensitive to small changes in those parameters. The steep slopes in Fig. 6 are a reflection of a recovery process that is increasingly controlled by diffusion on the cell body rather that on the tether.

If the more complete theoretical description given by Eqs. 3–5 is to be applied, then Fig. 6 gives some indication that protein mobility on the cell body may be somewhat enhanced over the nominal value of 4×10^{-11} cm^2/s. The shaded region in the figure corresponds to the expected range of values for D_T and R_T. The upper bound for D_T is taken to be $\sim 10^{-8}$ cm^2/s because this is the fastest rate measured for lipid probes diffusing in red cell membranes (Koppel et al., 1981; Bloom and Webb, 1983). The true tether radius is probably at the upper end of the range, based on the previously mentioned electron micrographic evidence, so it would appear that the effective cell body diffusivity is $>6 \times 10^{-11}$ cm^2/s. This may be the consequence of enhanced diffusivity in the neck region due to incipient membrane failure.

DISCUSSION

The experiments described here have taken advantage of the geometry of the cell body and its tether to accomplish a FRAP measurement without the considerable expense of laser illumination. An average tether contains approximately the same membrane surface area as a 1-μm radius spot on the cell body. Whereas the tether can be selectively illuminated by a conventional light source, the spot on the cell body must be illuminated by a precisely focused laser. Unfortunately, the versatility of a laser-based FRAP system is indispensable for resolving the related issues that arise. Clearly, had one been available, a laser-based FRAP system would have been useful to make more accurate measurements of diffusion on the cell body, as well as to photobleach small portions of the tether to achieve a situation that is even more independent of diffusion on the cell body. Laser illumination would also have allowed the measurement of diffusion coefficients and %R on the tether and body of the same cell. However, the result achieved with arc lamp illumination is clear enough: the fluorescence recoveries are consistent with

a tether membrane diffusion coefficient greater than 10^{-9} cm^2/s.

If protein diffusion in the tether is truly unconstrained, then one would expect that the diffusion of a fluorescent lipid analogue from the cell body to tether measured by the same technique would be only slightly faster. Unfortunately, this confirmational experiment could not be performed with the apparatus described in this paper for several reasons. The lipid analogue DiI was incorporated into red blood cells, and fluorescent tethers were then created and observed. Compared to the fluorescein-based protein dye, DiI is exceedingly resistant to photobleaching. The exposure time required to achieve significant bleaching with this apparatus is comparable to the expected recovery time. The concept of an instantaneous bleach followed by an unimpeded recovery is no longer remotely applicable. Additionally, the photomultiplier tube detector exhibited a poor response to the longer wavelength fluorescence of the lipid analogue. This meant that the fluorescence recovery after a brief bleach was almost completely obscured by noise. Experiments with a fluoresceinated Phosphatidyl ethanolamine resulted in relatively poor incorporation into the red cell membrane and an inadequate signal.

Although a theoretical description has been derived to describe the diffusion from a spherical surface to a cylindrical projection, the experiments presented here are certainly not complete enough to form a test of the theory. Undoubtably, the most convincing demonstration of its applicability would be a series of experiments in which the diffusion coefficients are known independently and the effect of changing a single dimension such as tether length can be thoroughly investigated. For this purpose, the use of artificial lipid bilayer vesicles containing a fluorescent lipid analogue is to be preferred to the red blood cell. With the lipid vesicle, the diffusion coefficients of cell body and tether would be identical, and there would be no complications related to an immobile fraction of fluorescent material. As suggested by the above comments regarding lipid fluorophores, this sort of experiment would require a more powerful light source (i.e., a laser) and preferably a more sensitive light detector than described in this paper.

The major finding of these experiments is that fluorescently labeled membrane components which normally exhibit restricted mobility are highly mobile in the membrane of red blood cell tethers. Measurements of protein mobility in normal erythrocyte membrane have consistently demonstrated a highly restricted diffusion coefficient $<10^{-10}$ cm^2/s (Peters et al., 1974; Fowler and Branton, 1977; Golan and Veatch, 1980). The minimum tether diffusion coefficient reported here is 1.5×10^{-9} cm^2/s, and the actual coefficient may be several times

greater. This mobility is comparable to that reported by Sheetz et al. (1980) for spectrin-deficient mouse erythrocytes and by Golan and Veatch (1980) for heat- and low-ionic-strength treated human erythrocytes. This coefficient is also comparable to those reported for protein diffusion on membrane blebs in a variety of cells (Tank et al., 1982; Wu et al., 1982; Barak and Webb, 1982).

The rapid diffusion measured for the tether raises the concern that the diffusing species is some component other than integral membrane proteins. Schindler et al. (1980) showed that DTAF labels primarily band 3 and glycophorin, with negligible labeling of lipid and hemoglobin. Our own studies show no reduction in fluorescence intensity after a cell is lysed, an indication that hemoglobin is not significantly labeled. Also, the tether has a much greater surface area to volume ratio than the cell as a whole, which would further reduce any contribution by cytoplasmic contents to the tether fluorescence intensity. A cytoplasmic component would diffuse through the bulk solution within the hollow tether with a coefficient on the order of 10^{-7} cm^2/s, which corresponds to a tether fluorescence recovery on the order of 10 s, 100× faster than observed. Finally, the measurement, by means of half-cell photobleaching, of very slow diffusion on the cell body confirms that integral membrane proteins are the major diffusing species.

Alternatively, the results could indicate that the major integral proteins, band 3 and glycophorin A, are excluded from the tether during its formation. The initial tether fluorescence and the subsequent recovered fluorescence would then arise solely from the unidentified labeled component (Schindler et al., 1980). If this component were highly mobile, its contribution to fluorescence recovery would be negligible in normal membrane but obvious in tether membrane where it would be the major fluorescent component. Thus the fast tether fluorescence recovery could indicate a difference in tether membrane composition apart from the presence or absence of cytoskeletal constraints upon mobility. For instance, this situation could arise if band 3 were excluded from regions of high membrane curvature and, conversely, the presence of the minor component were favored by high curvature.

This alternate explanation does not seem likely, though it cannot be ruled out. If the great majority of the fluorescently labeled particles were excluded from the tether, then that would be reflected in the comparative fluorescence intensities of the tether membrane and cell body membrane. However, there are a number of difficulties in determining the relative surface densities of fluorescent particles on the cell body and tether. First, the video camera and processing system were not calibrated, although the camera specifications claim it

responds linearly to image intensity. Second, the intensity of a fluorescent fiber with diameter on the order of one light wavelength cannot be directly compared with the intensity of a large planar fluorescence source. The diffraction pattern created by such a thin fluorescent strand depends on the fiber thickness and on the microscope optics (numerical aperture of the objective). In videomicrographs of the fluorescent cell with its tether (Fig. 2), the tether intensity is always less than the cell body intensity but still much greater than the background intensity. This would seem to indicate that the tether surface density of fluorescent material is not radically depleted compared to the cell body. Further investigation, with the use of other fluorescent labels and a well calibrated photometric video image analysis system, will be needed to resolve this concern.

The unconstrained diffusion on the tether membrane rules out the possibility shown in Fig. 1 a that membrane rearranges as it flows, to form normal membrane again. Spectrin may well be completely absent from the tether membrane. If there are any vestiges of the cytoskeletal network in the tether, it is difficult to estimate the extent of disruption necessary to release the constraints on lateral mobility. As yet there is no complete understanding of the mechanism by which the superficial cytoskeletal network restricts protein mobility in the lipid bilayer. One view is that the spectrin network creates a physical barrier to the motion of integral proteins, so that long-range motion depends on the fluctuations of those transient barriers. This model is not supported by experimental studies of some integral proteins (not erythrocyte proteins) that showed the restriction in lateral mobility is independent of the size of the protein's cytoplasmic domain (Edidin and Zuniga, 1984; Livneh et al., 1986). Another possible mechanism for the restriction of mobility is the transient binding of the integral protein to an element of the cytoskeleton, either directly or through a second integral protein in the bilayer (Golan, 1989). Until the mechanism for restriction of lateral mobility is better understood, it will be difficult to directly relate membrane mechanical properties to mobility of integral proteins. Saxton (1990) has proposed a model for the red cell membrane that explicitly relates membrane shear elasticity with long-range diffusion of proteins. The general feature of the model is that unconstrained diffusion is accompanied by a breakdown of elasticity, but the nature of transition from restricted to unconstrained mobility is governed by the timescale of the transient barriers created by the cytoskeleton.

In these experiments, the completely unconstrained mobility of the fluorescent proteins in the tether implies that the membrane flow process involves the removal or
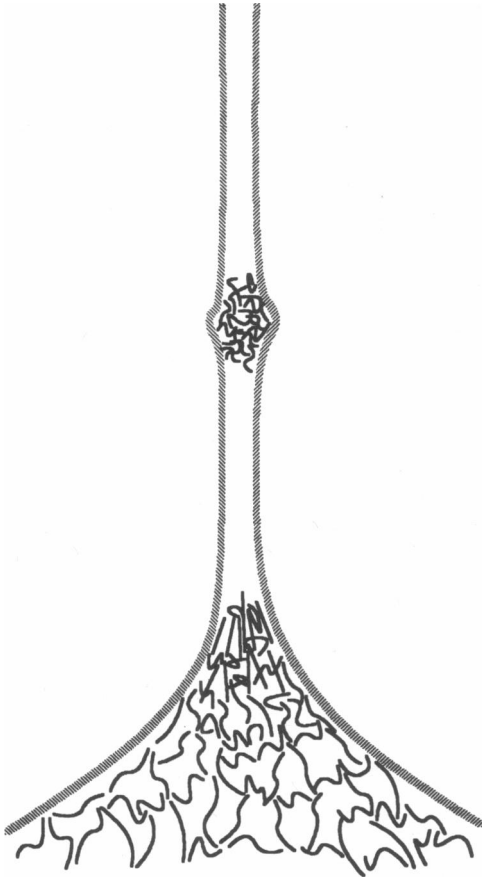
FIGURE 7 Speculative model for extensional failure. The observed flow of material involves separation of the lipid bilayer from the protein matrix. The resulting tether membrane is deficient in cytoskeletal proteins. Fragments of cytoskeletal material may flow onto the tether and form globules in the lipid bilayer cylinder.

denaturation of the cytoskeleton and the consequent loss of membrane shear elasticity. These results support a model of the tether as a hollow cylinder of lipid bilayer (Waugh and Hochmuth, 1987). Furthermore, this evidence provides an impetus for reinterpreting past experiments that measured yield shear and "plastic viscosity" of membrane flow from cell body to tether. The flow process should be modeled as a multilamellar phenomenon in which the lipid bilayer flows as a two-dimensional liquid but the solidlike cytoskeletal layer is fragmented or completely separated from the lipid bilayer. Fig. 7 shows one possible model in which the lipid bilayer flows over the cytoskeletal elements. The cytoskeletal proteins collect in the neck region, but may also form clumps that flow with the lipid and can be observed as globular regions within the tether.

REFERENCES

Barak, L. S., and W. W. Webb. 1982. Diffusion of low density lipoprotein-receptor complex on human fibroblasts. *J. Cell Biol.* 95:846–852.

Bennett, V. 1985. The membrane skeleton of human erythrocytes and its implications for more complex cells. *Annu. Rev. Biochem.* 54:273–304.

Berk, D., A. Clark, and R. M. Hochmuth. 1992. Analysis of lateral diffusion from a spherical cell surface to a tubular projection. *Biophys. J.* 61:1–8.

Bloom, J. A., and W. W. Webb. 1983. Lipid diffusibility in the intact erythrocyte membrane. *Biophys. J.* 42:295–305.

Edidin, M., and M. Zuniga. 1984. Lateral diffusion of wild type and mutant L^d antigens in L cells. *J. Cell Biol.* 99:2333–2335.

Evans, E. A., and R. M. Hochmuth. 1976a. Membrane viscoelasticity. *Biophys. J.* 16:1–11.

Evans, E. A., and R. M. Hochmuth. 1976b. Membrane viscoplastic flow. *Biophys. J.* 16:13–26.

Fowler, V., and D. Branton. 1977. Lateral mobility of human erythrocyte integral membrane proteins. *Nature (Lond.).* 268:23–26.

Golan, D. E. 1989. Red blood cell membrane protein and lipid diffusion. *In* Red Blood Cell Membranes: Structure, Function, Clinical Implications. P. Agre and J. C. Parker, editors. Marcel Dekker, Inc., New York.

Golan, D. E., and W. Veatch. 1980. Lateral mobility of band 3 in the human erythrocyte membrane studied by fluorescence photobleaching recovery: evidence for control by cytoskeletal interactions. *Proc. Natl. Acad. Sci. USA.* 77:2537–2541.

Hochmuth, R. M., and E. A. Evans. 1982. Extensional flow of erythrocyte membrane from cell body to elastic tether. I. Analysis. *Biophys. J.* 39:71–81.

Hochmuth, R. M., N. Mohandas, and P. L. Blackshear. 1973. Measurement of the elastic modulus for red cell membrane using a fluid mechanical technique. *Biophys. J.* 13:747–762.

Hochmuth, R. M., E. A. Evans, and D. F. Colvard. 1976. Viscosity of human red cell membrane in plastic flow. *Microvasc. Res.* 11:155–159.

Hochmuth, R. M., H. C. Wiles, E. A. Evans, and J. T. McCown. 1982. Extensional flow of erythrocyte membrane from cell body to elastic tether. II. Experiment. *Biophys. J.* 39:83–89.

Hochmuth, R. M., E. A. Evans, H. C. Wiles, and J. T. McCown. 1983. Mechanical measurement of red cell membrane thickness. *Science (Wash. DC).* 220:101–102.

Huang, H. W. 1973. Mobility and diffusion in the plane of cell membrane. *J. Theor. Biol.* 40:11–17.

Koppel, D. E., M. P. Sheetz, and M. Schindler. 1981. Matrix control of protein diffusion in biological membranes. *Proc. Natl. Acad. Sci. USA.* 78:3576–3580.

Livneh, E., M. Benveniste, R. Prywes, S. Felder, Z. Kam, and J.

Schlessinger. 1986. Large deletions in the cytoplasmic kinase domain of the epidermal growth factor receptor do not affect its lateral mobility. *J. Cell Biol.* 103:327–331.

Markle, D. R., E. A. Evans, and R. M. Hochmuth. 1983. Force relaxation and permanent deformation of erythrocyte membrane. *Biophys. J.* 42:91–98.

Peters, R. J., J. Peters, K. H. Tews, and W. Bahr. 1974. A microfluorimetric study of translational diffusion in erythrocyte membranes. *Biochim. Biophys. Acta.* 367:282–294.

Saxton, M. J. 1989. The spectrin network as a barrier to lateral diffusion in erythrocytes. A percolation analysis. *Biophys. J.* 55:21–28.

Saxton, M. J. 1990. The membrane skeleton of erythrocytes. A percolation model. *Biophys. J.* 57:1167–1177.

Schindler, M., D. E. Koppel, and M. P. Sheetz. 1980. Modulation of membrane protein lateral mobility by polyphosphates and polyamines. *Proc. Natl. Acad. Sci. USA.* 77:1457–1461.

Sheetz, M. P., M. Schindler, and D. E. Koppel. 1980. Lateral mobility of integral membrane proteins is increased in spherocytic erythrocytes. *Nature (Lond.).* 285:510–512.

Smith, D. A., and J. Palek. 1982. Modulation of lateral mobility of band 3 in the red cell membrane by oxidative cross-linking of spectrin. *Nature (Lond.).* 297:424–425.

Tank, D. W., E. S. Wu, and W. W. Webb. 1982. Enhanced molecular diffusibility in muscle membrane blebs: release of lateral constraints. *J. Cell Biol.* 92:207–212.

Waugh, R. E. 1982. Temperature dependence of the yield shear resultant and plastic viscosity coefficient of erythrocyte membrane: Implications about molecular events during membrane failure. *Biophys. J.* 39:273–278.

Waugh, R. E., and P. Agre. 1988. Reductions of erythrocyte membrane viscoelastic coefficients reflect spectrin deficiencies in hereditary spherocytosis. *J. Clin. Invest.* 81:133–141.

Waugh, R. E., and R. M. Hochmuth. 1987. Mechanical equilibrium of thick, hollow, liquid membrane cylinders. *Biophys. J.* 52:391–400.

Webb, W. W., L. S. Barak, D. W. Tank, and E. S. Wu. 1981. Molecular mobility on the cell surface. *Biochem. Soc. Symp.* 46:191–205.

Wu, E. S., D. W. Tank, and W. W. Webb. 1982. Unconstrained lateral diffusion of concanavalin A receptors on bulbous lymphocytes. *Proc. Natl. Acad. Sci. USA.* 79:4962–4966.